

Numerical Investigation of Microjet Impingement of Water for Cooling Photovoltaic Solar Cell

Open
Access

Husam Abdulrasool Hasan^{1,*}, Kamaruzzaman Sopian², Kayser Aziz Ameen¹

¹ Department of Air Conditioning and Refrigeration Engineering, Al Esra'a University College, Baghdad, Iraq

² Solar Energy Research Institute, Universiti Kebangsaan Malaysia, 43600 Bangi, Selangor, Malaysia

ARTICLE INFO

ABSTRACT

Article history:

Received 2 July 2018

Received in revised form 15 October 2018

Accepted 19 October 2018

Available online 6 November 2018

Keywords:

Photovoltaic solar cell, Numerical studies, jet impingement, Nusselt numbers, nozzle diameter

This paper discussed the results of numerical studies of the flow field and heat transfer characteristics for a turbulent slot jet of water on photovoltaic solar cell. A wide range of various flow and geometrical parameters, with jet Reynolds number (Re) in the range of 10000-30000, and jet-to-photovoltaic distance (h) and the nozzle diameter have been considered. The results have been presented in terms of the average Nusselt numbers, and the heat transfer coefficients. The results show a significant improvement of heat transfer due to the jet impingement of water for cooling photovoltaic solar cell. An increase in the jet Reynolds number leads to an improved average Nusselt numbers increases as the nozzle-to-photovoltaic spacing decreases.

Copyright © 2018 PENERBIT AKADEMIA BARU - All rights reserved

1. Introduction

Impinging cooling is an effective way to generate a high heat transfer coefficient in many engineering applications such as cooling of electronic equipment, drying of surfaces, cooling of turbine blades, laser or plasma cutting processes and steel or glass industry [1–4]. They measured free surface velocities by using the Laser-Doppler technique. The Reynolds number changing from 16,000 to 47,000 in the experimental test. Liu *et al.*, [6] studied experimentally and numerically the cooling of uniformly heated surfaces with single phase jets and laminar circular liquid. Kazuya *et al.*, [7] studied experimentally the influence of varying the impingement angles between the vertical planar jet and the inclined solid surface on the heat transfer characteristics of a planar free water jet impinging onto a flat substrate. The planar jet of a rectangular slot nozzle with cross section of 1.62 mm 40 mm was tested. The range of Reynolds number ranging from 2200 to 8800 based on the nozzle gap and the mean velocity. Teamah and his coworkers [8–11] investigated the heat transfer due to the impingement of circular jet on a horizontal heated surface. They tested single and multi-jets experimentally and numerically. The flow rates of water ranging from 1.5 to 8 l/min per jet. They

* Corresponding author.

E-mail address: hussam2003hussam@yahoo.com

observed that, the jets lead to reduce the mean velocity of the fluid film for multi jets, which led to reduce of both the average local and local Nusselt number compared to the single jet. It was also noted that the overall average Nusselt number for multi jet is higher than single jet of one jet of the multi jets. Stevens and Webb [12] studied experimentally the influence of jet inclination on the local heat transfer under an obliquely impinging, round; free liquid jet striking a constant heat flux surface. The jet Reynolds number ranging from 6600 to 52,000, and jet inclination, ranging from 40 to 90. They observed that the point of maximum heat transfer shifted upstream. Whelan and Robinson [13] tested experimentally the average heat transfer coefficients and pressure drop of both impinging confined-submerged and free surface water jet arrays. Dou *et al.*, [14] investigated the heat-transfer characteristics of the water jet on stainless steel flat plates with using inverse heat conduction methods. Karwa and Stephan [15] studied experimentally the thermo-hydrodynamic phenomenon of a hot stainless steel flat plates. The stainless steel flat plates were heated at an initial temperature of 900°C, with a free-surface sub-cooled water jet. Lytle and Webb [16] investigated experimentally the local heat transfer characteristic by using an infrared thermal imaging technique. They found that the local Nusselt number increases as the nozzle-to-plate spacing decreases when the Reynolds number fix. A power-law relationship between the stagnation Nusselt number and the jet-to-target distance was presented. Choo *et al.*, [17,18] studied the heat transfer characteristics of impinging jet with fixing pumping power condition at low nozzle-to-plate distance. They observed that the average Nusselt number is independent of the nozzle-to-plate spacing with fixed pumping power condition. Lee *et al.*, [19] investigated experimentally the influence of nozzle diameter on fluid flow and heat transfer for a round turbulent jet at nozzle-to-plate distance from $H/d = 2$ to 14. The maximum Nusselt number can be achieved when $H/d = 7$ where the turbulence intensity reaches roughly a maximum value. Gardon and Akfirat [20,21] found that the variation of the stagnant Nusselt number is negligible to the hump. It decreases beyond the hump. The hump moves from $H/d = 6$ to 2 as the Reynolds number increases.

2. Mathematical Model and Numerical Solution

2.1 Governing Equations

Figure 1 shows a schematic diagram of the geometry and the computational domain used in the present work. According to the geometrical dimensions chosen in the experimental study. The different nozzle diameters (d) 0.6, 0.8, 1.0 and 1.5 mm have been considered. In addition, the photovoltaic surface which is subjected to a constant heat flux, has negligible thickness, and is stationary. In this problem, a steady and turbulent two-dimensional flow is considered. It is also assumed that the working fluid (water) is Newtonian and incompressible. In view of the above assumptions, the governing equations of the problem are the continuity, momentum, and energy equations and the transport equations for the turbulent kinetic energy and its dissipation rate.

$$\frac{\partial U_i}{\partial x_i} = 0 \quad (1)$$

$$\rho U_i \frac{\partial U_i}{\partial x_i} = -\frac{\partial P}{\partial x_i} + \frac{\partial}{\partial x_i} \left[\mu \left(\frac{\partial U_i}{\partial x_j} + \frac{\partial U_j}{\partial x_i} \right) - \rho \overline{u'_i u'_j} \right] \quad (2a)$$

$$-\rho \overline{u'_i u'_j} = \mu_t \left(\frac{\partial U_i}{\partial x_j} + \frac{\partial U_j}{\partial x_i} \right) - \frac{2}{3} \delta_{ij} \rho k \quad (2b)$$

$$\rho C_p U_i \frac{\partial T}{\partial x_i} = \frac{\partial}{\partial x_i} \left[k \frac{\partial T}{\partial x_i} - \rho \overline{u_i' T'} \right] \quad (3)$$

The turbulent viscosity term μ_t is to be computed from an appropriate turbulence model. The expression for the turbulent viscosity is given as

$$\mu_t = \rho C_\mu \frac{K^2}{\varepsilon} \quad (4)$$

In the present study, k- ε RNG turbulence model is used as follows

$$\frac{\partial}{\partial x_i} (\rho k u_i) = \frac{\partial}{\partial x_j} \left[\left(\mu + \frac{\mu_t}{\sigma_k} \right) \frac{\partial k}{\partial x_j} \right] + G_k - \rho \varepsilon \quad (5)$$

Similarly, the dissipation rate of TKE, ε is given by the following equation.

$$\frac{\partial}{\partial x_i} (\rho \varepsilon u_i) = \frac{\partial}{\partial x_j} \left[\left(\mu + \frac{\mu_t}{\sigma_\varepsilon} \right) \frac{\partial \varepsilon}{\partial x_j} \right] + C_{1\varepsilon} \frac{\varepsilon}{k} G_k - C_{2\varepsilon} \rho \frac{\varepsilon^2}{k} \quad (6)$$

Where G_k is the rate of generation of the TKE while $\rho \varepsilon$ is the destruction rate. G_k is written as

$$G_k = (-\overline{\rho u_i' u_j'}) \frac{\partial u_j}{\partial x_i} \quad (7)$$

2.2 Boundary Conditions

The boundary conditions applied in the present work are illustrated in Figure 1. As shown in this figure, a velocity-inlet boundary condition at constant temperature (298 K) is assumed at the jet exit with a velocity magnitude compatible with the jet exit Reynolds number. The inlet turbulence intensity and hydraulic diameter were set to be 5% and 2d respectively. The thermal boundary condition at the photovoltaic surface is a constant heat flux. Also, at the flow outlet, the pressure-outlet boundary condition has been assumed

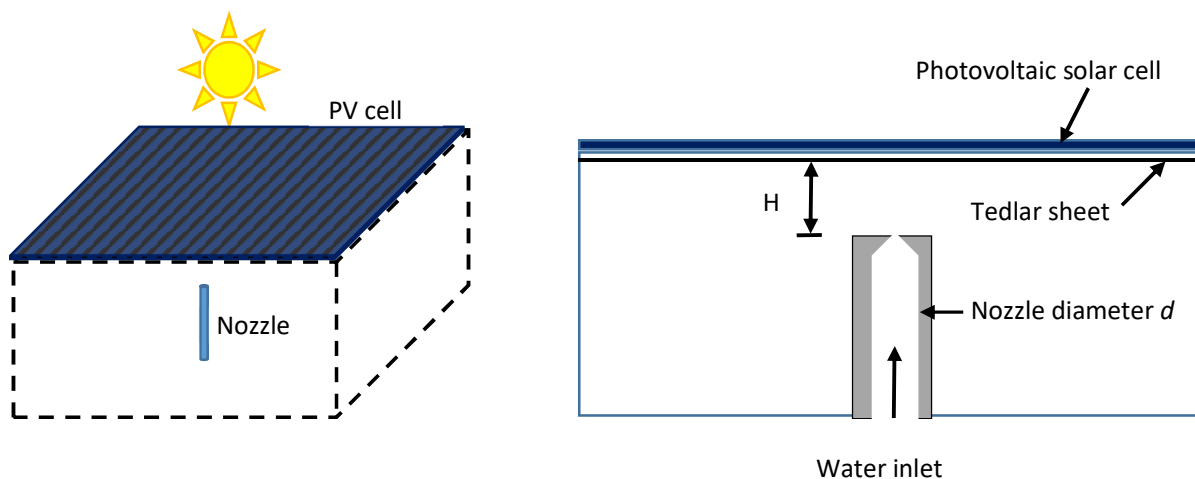


Fig. 1. Schematic of slot-jet impingement cooling scheme on photovoltaic solar panel

To attain accurate prediction in the circular tube, the standard $k - \varepsilon$ turbulence model, the Renormalized Group (RNG) $k - \varepsilon$ turbulence model were selected. The time-independent incompressible Navier-Stokes equations and the turbulence model analysis were solved using finite volume method. To evaluate the pressure field, the pressure-velocity coupling algorithm SIMPLE (Semi Implicit Method for Pressure-Linked Equations) was selected. The solutions are considered to be converged when the normalized residual values reach 10^{-5} for all variables.

3. Results and Observations

3.1 Effect of Nozzle Photovoltaic Cell Spacing

The numerical study was conducted to study the effect of jet impingement of water for cooling photovoltaic solar cells. The different nozzle-to- photovoltaic spacing of 10, 20, 30 and 40mm was studied with different Reynolds number at different nozzles size. Figure 2 shows the variation of Nusselt number with Reynolds number. From the results, it is clearly noted that the Nusselt number increases with the rise of Reynolds number for all spacing. The Nusselt number also increases with the decrease of the nozzle-to- photovoltaic spacing and has a maximum value at the spacing of 10mm for $d=0.6$ case. This can be explained by a high heat transfer coefficient and rapid mixing flow can be achieved when the photovoltaic solar cell closes to the nozzle.

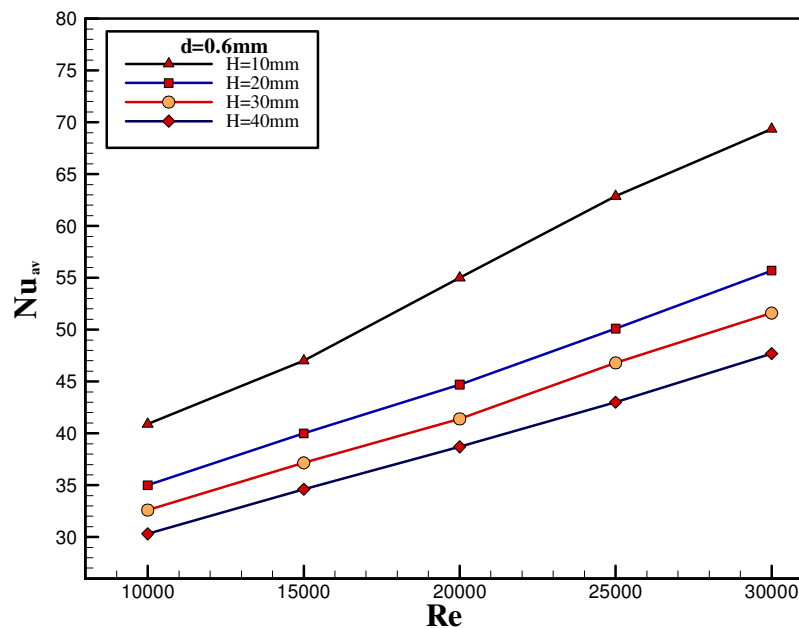


Fig. 2. Variation of the Nusselt number with Reynolds number for different nozzle-to- photovoltaic cell spacing at $d=0.6$ mm

Figure 3 shows the variation of Nusselt with Reynolds numbers at different nozzle-to- photovoltaic cell spacing of 10, 20, 30 and 40mm at $d=0.8$ mm. It is observed that the Nusselt number increases with the rise of Reynolds number for all spacing. The Nusselt number also increases with the decrease of the nozzle-to- photovoltaic cell spacing. It can be seen that the high values of average Nusselt number occur in the jet impingement the nozzle-to- photovoltaic cell spacing is 10mm.

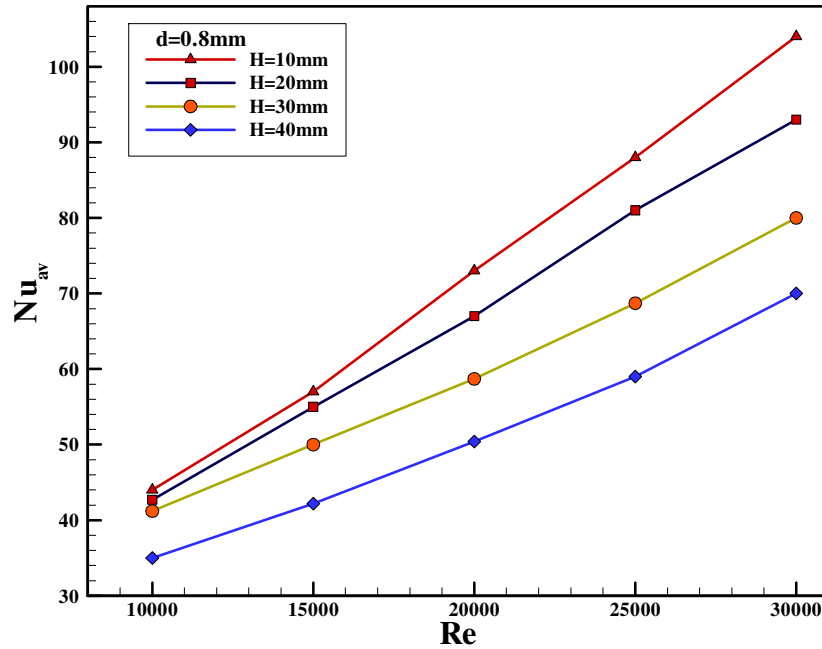


Fig. 3. Variation of the Nusselt number with Reynolds number for different nozzle-to-photovoltaic spacing at $d=0.8mm$

Figure 4 shows the variation of Nusselt number with Reynolds number at different nozzle-to-photovoltaic spacing of 10,20,30 and 40mm at $d=1mm$. As can be seen from this figure, increasing the jet Reynolds number, will increase the inlet velocity. This will lead to the average Nusselt number increase significantly. The Nusselt number also increases with the decrease of the nozzle-to-photovoltaic spacing. It can be seen that the high values of average Nusselt number occur in the jet impingement the nozzle-to- photovoltaic spacing at 10mm.

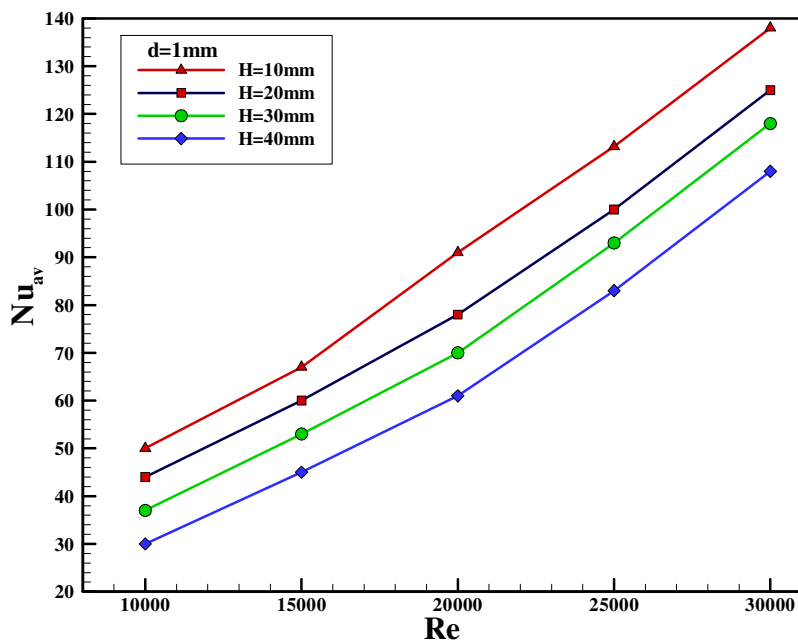


Fig. 4. Variation of the Nusselt number with Reynolds number for different nozzle-to-photovoltaic cell spacing at $d=1mm$

Figure 5 shows the variation of Nusselt number with Reynolds number at different nozzle-to-photovoltaic spacing of 10,20,30 and 40mm at $d=1.5\text{mm}$. From the results, it is clearly noted that the Nusselt number increases with the rise of Reynolds number for all spacing. The Nusselt number also increases with the decrease of the nozzle-to- photovoltaic spacing and has a maximum value at the spacing of 10mm for $d=1.5$ case. This can be explained by a high heat transfer coefficient and rapid mixing flow can be achieved when the photovoltaic solar cell is close to the nozzle.

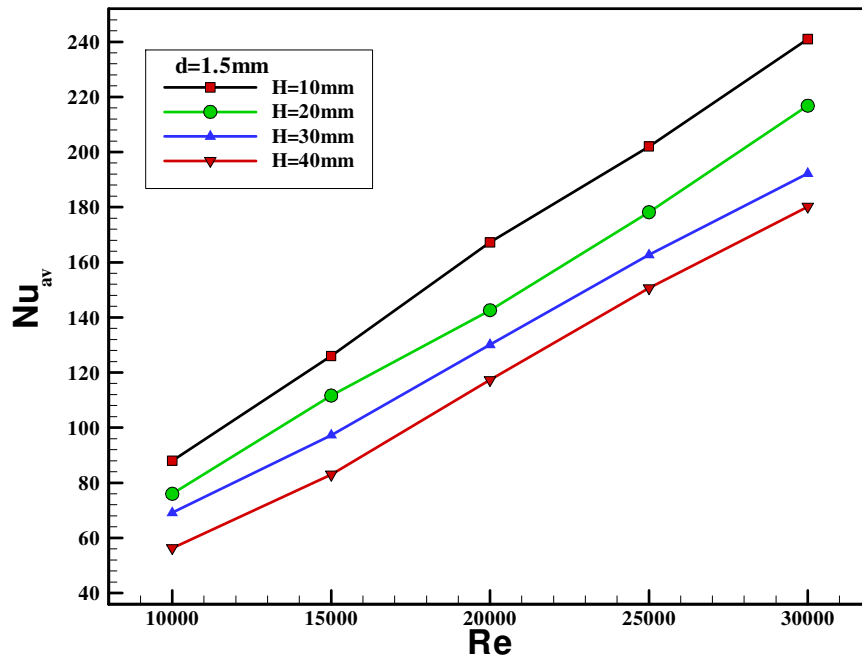


Fig. 5. Variation of the Nusselt number with Reynolds number for different nozzle-to-photovoltaic cell spacing at $d=1.5\text{mm}$

3.2 Effect of Nozzle Diameter

Figure 6 shows the variation of the Nusselt number with Reynolds number for different nozzle diameter at $H=10\text{mm}$. According to the results, it is clearly seen that the Nusselt number increases with the rise of Reynolds number for all nozzle diameter. The Nusselt number also increases with the increase of the nozzle diameter and has a maximum value at the $d=1.5$.

3.3 Effect of Different Reynolds Number on The Local Heat Transfer Coefficient

Figure 7 shows the variation of local heat transfer coefficient with $X(\text{m})$ at different Reynolds number with nozzle-to- photovoltaic spacing of 10mm at $d=0.8\text{mm}$. From the results, it is clearly noted that the heat transfer coefficient increases with the rise of Reynolds number. Figure 8 shows the variation of heat transfer coefficient with $X(\text{m})$ at different Reynolds number with nozzle-to-photovoltaic spacing of 10mm at $d=1.5\text{mm}$. From the results, it is clearly shown that the heat transfer coefficient increases with the rise of Reynolds number.

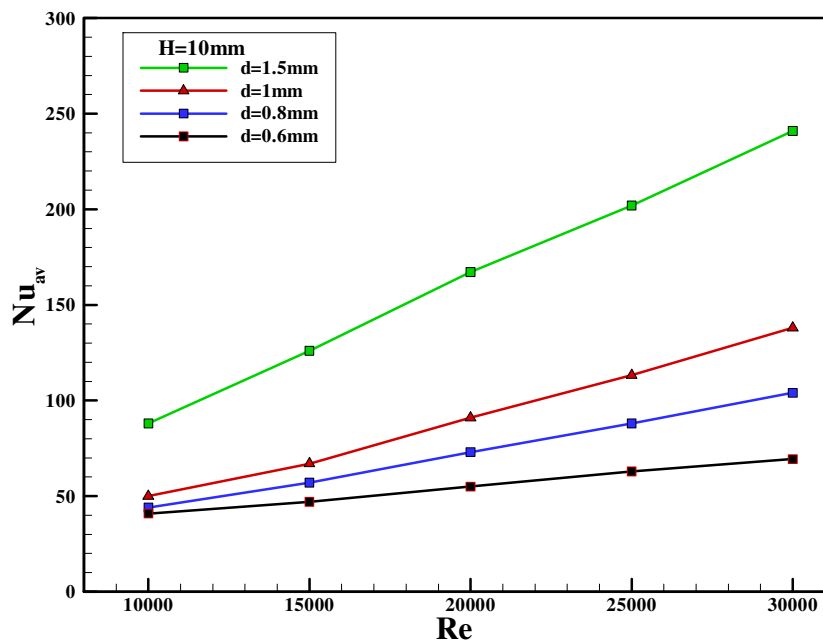


Fig. 6. Variation of the Nusselt number with Reynolds number for different nozzle diameter at H=10mm

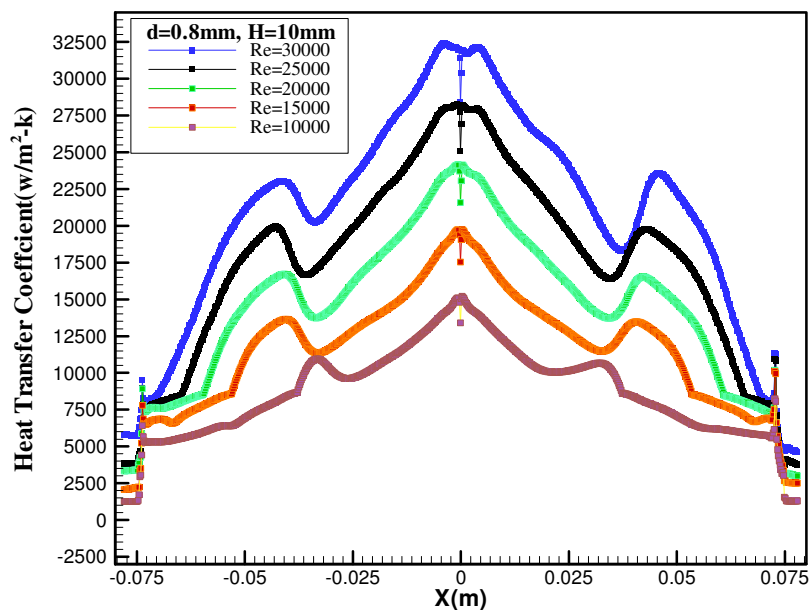


Fig. 7. Variation of the local heat transfer coefficient with X at d=0.8 mm and H=10mm

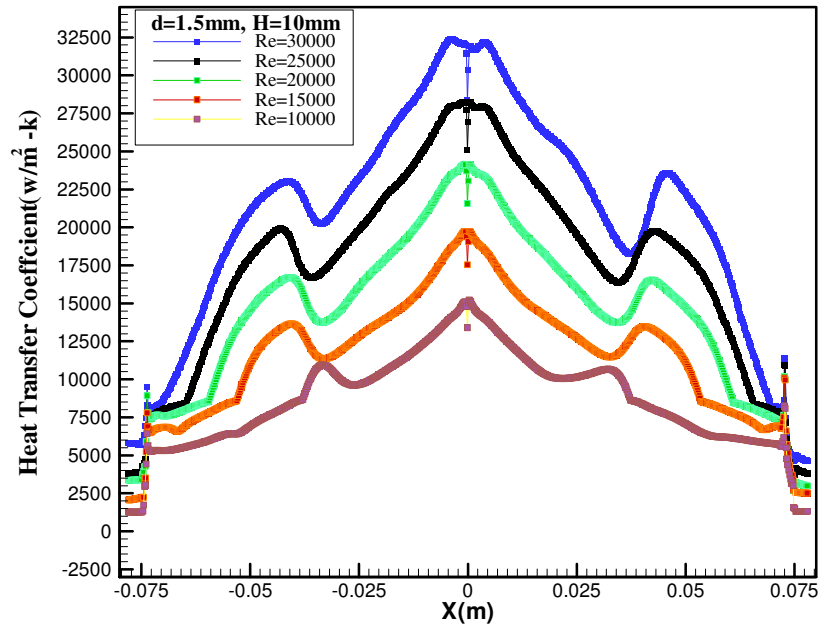


Fig. 8. Variation of the heat transfer coefficient with X at d=0.8 mm and H=10mm

4. Conclusions

The effects of using jet impingement of water on the heat transfer field due to cooling a photovoltaic solar cell were numerically analysed. The impacts of the nozzle diameter, Reynolds numbers, and jet-to- photovoltaic distances on the heat transfer of jet water have been discussed in detail. The outcomes indicate that by increasing the jet Reynolds number and decreasing the jet-to-target space, the target surface temperature is reduced which results in enhancement of the average Nusselt number distribution. Hence, the average Nusselt numbers increase as the nozzle increases. It is also found that the average Nusselt numbers increases as the nozzle-to-photovoltaic spacing decreases because jet Reynolds number increasing led to increase the heat transfer coefficients. Also, it is clearly noted that the heat transfer coefficient increases with the rise of Reynolds number. The Nusselt number considerably increased with increasing Reynolds number, Re in the range of 10000-30000.

Acknowledgements

The authors would like to thank the Universiti Kebangsaan Malaysia (UKM) for funding (DPP-2018-002), and Al-Esra'a University.

References

- [1] Afroz, Farhana, and M. A. R. Sharif. "Numerical study of heat transfer from an isothermally heated flat surface due to turbulent twin oblique confined slot-jet impingement." *International Journal of Thermal Sciences* 74 (2013): 1-13.
- [2] Narumanchi, Sreekant VJ, Cristina H. Amon, and Jayathi Y. Murthy. "Influence of pulsating submerged liquid jets on chip-level thermal phenomena." *Journal of Electronic Packaging* 125, no. 3 (2003): 354-361.
- [3] Fabbri, Matteo, Shanjuan Jiang, and Vijay K. Dhir. "Experimental investigation of single-phase micro jets impingement cooling for electronic applications." In *ASME 2003 Heat Transfer Summer Conference*, pp. 461-468. American Society of Mechanical Engineers, 2003.

- [4] Hollworth, B. R., and M. Durbin. "Impingement cooling of electronics." *Journal of Heat Transfer* 114, no. 3 (1992): 607-613.
- [5] Stevens, J., and B. W. Webb. "Measurements of the free surface flow structure under an impinging, free liquid jet." *Journal of Heat Transfer* 114, no. 1 (1992): 79-84.
- [6] Liu, X., J. H. Lienhard, and J. S. Lombara. "Convective heat transfer by impingement of circular liquid jets." *Journal of heat transfer* 113, no. 3 (1991): 571-582.
- [7] Ibuki, Kazuya, Taichi Umeda, Hitoshi Fujimoto, and Hirohiko Takuda. "Heat transfer characteristics of a planar water jet impinging normally or obliquely on a flat surface at relatively low Reynolds numbers." *Experimental thermal and fluid science* 33, no. 8 (2009): 1226-1234.
- [8] Teamah, Mohamed A., and Sameh Farahat. "Experimental and numerical heat transfer from impinging of single free liquid jet." *Alexandria Engineering Journal* 42, no. 5 (2003): 559-575.
- [9] Teamah, M., and Sameh Farahat. "Experimental heat transfer due to impinging of water from multiple jets on a heated surface." *Alexandria Engineering Journal* 45, no. 1 (2006): 1-13.
- [10] Teamah, Mohamed A., M. Khalil Ibrahim, MM Khairat Dawood, and E. Abdel Aleem. "Experimental investigation for hydrodynamic flow due to obliquely free circular water jet impinging on horizontal flat plate." *European Journal of Scientific Research* 83, no. 1 (2012): 60-75.
- [11] Teamah, Mohamed A., and Mohamed M. Khairat. "Heat transfer due to impinging double free circular jets." *Alexandria Engineering Journal* 54, no. 3 (2015): 281-293.
- [12] Stevens, J., and B. W. Webb. "The effect of inclination on local heat transfer under an axisymmetric, free liquid jet." *International Journal of Heat and Mass Transfer* 34, no. 4-5 (1991): 1227-1236.
- [13] Whelan, Brian P., and Anthony J. Robinson. "Nozzle geometry effects in liquid jet array impingement." *Applied Thermal Engineering* 29, no. 11-12 (2009): 2211-2221.
- [14] Dou, Ruifeng, Zhi Wen, Gang Zhou, Xunliang Liu, and Xiaohong Feng. "Experimental study on heat-transfer characteristics of circular water jet impinging on high-temperature stainless steel plate." *Applied Thermal Engineering* 62, no. 2 (2014): 738-746.
- [15] Karwa, Nitin, and Peter Stephan. "Experimental investigation of free-surface jet impingement quenching process." *International Journal of Heat and Mass Transfer* 64 (2013): 1118-1126.
- [16] Lytle, D., and B. W. Webb. "Air jet impingement heat transfer at low nozzle-plate spacings." *International Journal of Heat and Mass Transfer* 37, no. 12 (1994): 1687-1697.
- [17] Choo, Kyo Sung, and Sung Jin Kim. "Heat transfer characteristics of impinging air jets under a fixed pumping power condition." *International Journal of Heat and Mass Transfer* 53, no. 1-3 (2010): 320-326.
- [18] Choo, Kyo Sung, and Sung Jin Kim. "Comparison of thermal characteristics of confined and unconfined impinging jets." *International Journal of Heat and Mass Transfer* 53, no. 15-16 (2010): 3366-3371.
- [19] Lee, D. H., Y. S. Chung, and D. S. Kim. "Turbulent flow and heat transfer measurements on a curved surface with a fully developed round impinging jet." *International Journal of Heat and Fluid Flow* 18, no. 1 (1997): 160-169.
- [20] Gardon, Robert, and J. Cahit Akfirat. "Heat transfer characteristics of impinging two-dimensional air jets." *Journal of Heat Transfer* 88, no. 1 (1966): 101-107.
- [21] Gardon, Robert, and J. Cahit Akfirat. "The role of turbulence in determining the heat-transfer characteristics of impinging jets." *International journal of heat and mass transfer* 8, no. 10 (1965): 1261-1272.
- [22] Hasan, Husam Abdulrasool, Kamaruzzaman Sopian, Ahed Hameed Jaaz, and Ali Najah Al-Shamani. "Experimental investigation of jet array nanofluids impingement in photovoltaic/thermal collector." *Solar Energy* 144 (2017): 321-334.
- [23] Husam Abdulrasool Hasan, K. Sopian. "Experimental investigation on jet array SiO₂-water nanofluid impingement of photovoltaic/thermal collector" In *Journal of Nuclear Energy Science & Power Generation Technology* 6, no. 7 (2017): 33.
- [24] Jaaz, Ahed Hameed, Husam Abdulrasool Hasan, Kamaruzzaman Sopian, Abdul Amir H. Kadhum, Tayser Sumer Gaaz, and Ahmed A. Al-Amiery. "Outdoor Performance Analysis of a Photovoltaic Thermal (PVT) Collector with Jet Impingement and Compound Parabolic Concentrator (CPC)." *Materials* 10, no. 8 (2017): 888.
- [25] Husam Abdulrasool Hasan. "Improve the performance of parabolic trough solar collector by using SiO₂-water nanofluid" *The 3rd Engineering Science and Technology International Conference* 3 (2016).
- [26] Dezfouli, M. M. S., K. Sopian, Ali Najah Al-Shamani, Husam Abdulrasool Hasan, Azher M. Abed, A. M. Elbreki, B. Elhub, and Sohif Mat. "Energy saving potential of solar cooling systems in hot and humid region." (2006).
- [27] Sopian, K., Al-Shamani, A. N., Mat, S., Hasan, H. A., Abed, A. M., Dezfouli, M. M., Elbreki, A. M., Elhub, B. "Optimizing Nanofluids with the Optimum of Round Tube Design on the Performance of PVT Collector," *Proceeding of The 3rd Engineering Science and Technology* (2016).